Cell & Bioscience

CORRECTION

Open Access

Correction to: Integrating spatial transcriptomics with single-cell transcriptomics reveals a spatiotemporal gene landscape of the human developing kidney

Hongwei Wu[1,2†], Fanna Liu[2†], Yu Shangguan[1], Yane Yang[3], Wei Shi[1], Wenlong Hu[1], Zhipeng Zeng[1], Nan Hu[1], Xinzhou Zhang[1], Berthold Hocher[4], Donge Tang[1*], Lianghong Yin[2*] and Yong Dai[1,2,5*]

Correction to: Cell & Bioscience (2022) 12:80
https://doi.org/10.1186/s13578-022-00801-x

In the original version [1] of this article, in the result section, we have cited the Additional file 1: Fig. S2 to the corresponding content. However, the authors have inadvertently deleted Additional file 1: Fig. S2 and its legend by mistake. The correct Additional file 1: Fig. S2 and its legend are shown below.

The revised Additional file is published with this correction.

Additional file 1: Fig. S2.

The original article can be found online at https://doi.org/10.1186/s13578-022-00801-x.

†Hongwei Wu and Fanna Liu contributed equally to this work

*Correspondence: donge66@126.com; yin_yun@126.com; daiyong22@aliyun.com

[1] Clinical Medical Research Center, Guangdong Provincial Engineering Research Center of Autoimmune Disease Precision Medicine, Shenzhen Engineering Research Center of Autoimmune Disease, The Second Clinical Medical College of Jinan University, Shenzhen People's Hospital, Shenzhen 518020, Guangdong, China
[2] Institute of Nephrology and Blood Purification, The First Affiliated Hospital of Jinan University, Jinan University, Guangzhou 510632, China
Full list of author information is available at the end of the article

© The Author(s) 2022. **Open Access** This article is licensed under a Creative Commons Attribution 4.0 International License, which permits use, sharing, adaptation, distribution and reproduction in any medium or format, as long as you give appropriate credit to the original author(s) and the source, provide a link to the Creative Commons licence, and indicate if changes were made. The images or other third party material in this article are included in the article's Creative Commons licence, unless indicated otherwise in a credit line to the material. If material is not included in the article's Creative Commons licence and your intended use is not permitted by statutory regulation or exceeds the permitted use, you will need to obtain permission directly from the copyright holder. To view a copy of this licence, visit http://creativecommons.org/licenses/by/4.0/. The Creative Commons Public Domain Dedication waiver (http://creativecommons.org/publicdomain/zero/1.0/) applies to the data made available in this article, unless otherwise stated in a credit line to the data.

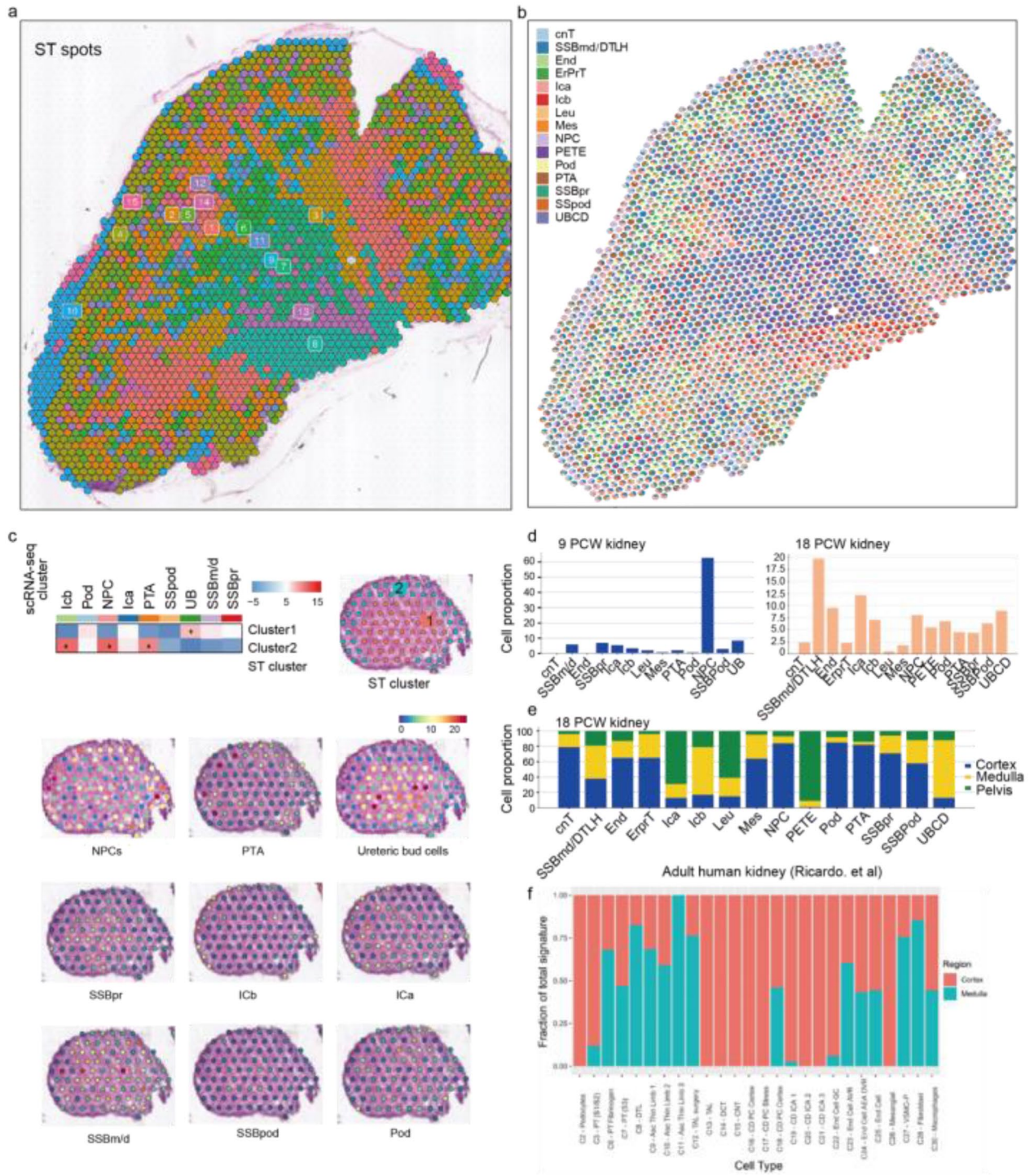

Figure S2. Cell-type deconvolution of the kidney tissues from 9 and 18 weeks post-conception. (a) Spatial location and clustering of ST-seq spots. (b) The proportion of signatures of different scRNA-seq cell types in each ST spot of the 18 PCW kidney tissue. Each pie chart represents the contribution of scRNA-seq cell types to the transcriptomic signature of each ST spot. Only cell types that contribute at least 10% to the spot signature are shown. (c) Up: multimodal intersection analysis (MIA) of scRNA-seq-identified cell types and ST-defined clusters. * represents the closest relationship between scRNA-identified

cell types and the ST-defined clusters ($P < 0.01$). Down: the spatial mapping of scRNA-seq cell subsets performed by MIA. (d) The proportion of each scRNA-seq cell subpopulation arising from each ST spot in the 9 and 18 PCW kidneys. (e) Fraction of total signature of each cell type present in the cortex, medulla, and pelvis in the 18 PCW kidney. (f) Fraction of total signature of each cell type present in the cortex, medulla, and pelvis in the adult human kidney (Ricardo et al.).

The original article has been corrected.

Supplementary Information

The online version contains supplementary material available at https://doi.org/10.1186/s13578-022-00878-4.

Additional file 1. Figure S1. scRNA-seq analysis of two human embryonic kidneys from 9 and 18 post-conception weeks. (a) Schematic of the experimental design and analysis. (b) Distribution of the number of transcripts and genes detected per spot at 9 and 18 PCW kidneys. Blue dashed lines indicate mean values, while the red dashed lines indicate the standard deviation. (c) Dimensionality reduction and clustering of the scRNA-seq data of the 9 and 18 PCW kidneys based on UMAP. (d) Quality control of the scRNA-seq data. ScRNA-seq dataset of fetal kidneys at 9 and 18 weeks post-conception are downloaded online (accession number: GSE114530). (e) Annotation of the cell types identified by spatial transcriptomics data based on the specific cell-type marker genes known from the literature. ST-seq, spatial transcriptomics sequencing; scRNA-seq, single-cell RNA sequencing; PCW, post-conception weeks; ICs, interstitial cells; PTA, pretubular aggregate; UBCD, ureteric bud/collecting duct; SSBmd/DTLH, distal tubule/loop of Henle and s-shaped body medial precursor cell; NPC, nephron progenitor cell; SSBpr, s-shaped body proximal precursor cell; ErprT, early proximal tubule. PETE, Pelvic segment transitional epithelium; Mes, mesangial cell; Pod, podocyte. **Figure S2.** Cell-type deconvolution of the kidney tissues from 9 and 18 weeks post-conception. (a) Spatial location and clustering of ST-seq spots. (b) The proportion of signatures of different scRNA-seq cell types in each ST spot of the 18 PCW kidney tissue. Each pie chart represents the contribution of scRNA-seq cell types to the transcriptomic signature of each ST spot. Only cell types that contribute at least 10% to the spot signature are shown. (c) Up: multimodal intersection analysis (MIA) of scRNA-seq-identified cell types and ST-defined clusters. * represents the closest relationship between scRNA-identified cell types and the ST-defined clusters ($P < 0.01$). Down: the spatial mapping of scRNA-seq cell subsets performed by MIA. (d) The proportion of each scRNA-seq cell subpopulation arising from each ST spot in the 9 and 18 PCW kidneys. (e) Fraction of total signature of each cell type present in the cortex, medulla, and pelvis in the 18 PCW kidney. (f) Fraction of total signature of each cell type present in the cortex, medulla, and pelvis in the adult human kidney (Ricardo et al.). **Figure S3.** Energy metabolism features of the renal cortex and medulla. Heatmaps displaying the expression levels of (a) OXPHOS-related genes and (b) glycolysis-related genes in scRNA-identified cell types in Hochane's study. (c) G2/M scores and mean expression levels of proliferation markers (Z-scores) per scRNA-identified cell subpopulation. This image is from Hochane's study. (d) The distribution feature of the dominated cell types in the cortical region of the 18 PCW kidney. (e) The distribution feature of the dominated cell types in the medullary region of the 18 PCW kidney. **Figure S4.** The biological function of the 16 distinct co-expressed patterns obtained from weighted gene co-expression network analysis. Left, diagrammatic drawing showing the relevance between the 16 modules and corresponding biological function. Scale bar: red represents a strong correlation, and gray indicates that the change in biological function did not reach the P-value threshold. Right, identification of biological function based on the differentially expressed genes in each module. **Figure S5.** Expression levels of M5 network genes for each (a) ST-seq and (b) scRNA-seq cell subpopulation. **Figure S6.** The expression of ribosome-related genes in NPC and PTA clusters identified in Hochane's study. The structure chart on the top left corner shows the spatial location of the NPC and PTA clusters. Violin plots showing the expression of ribosome-related genes in NPC and PTA clusters. **Figure S7.** Development of the nephric duct. (a) Schematic diagram showing the outgrowth of the UB and its regulatory network. UMPA showing the expression of regulatory genes controlling UB development in the 15 spatial cell clusters. (b) Matching plots show the significant signaling transduction regulation between NPC, PTA, and UB cells (score >0.5 and a $P < 10^{-4}$). pink represents the ligand, and blue represents the receptor in the ligand-receptor pairs. **Figure S8.** Maturation pathways and signaling in the developing kidneys. (a) Protein-protein network showing the correlation of the 366 up-regulated genes during NPC development (from the 8 PCW to 18 PCW kidneys). Genes involved in the common developmental pathways are marked with the same colors. Blue represents genes represent genes that have no significant pathways enrichment. (b) Cellular communication between NPC cluster and UB cluster in the 9 PCW kidney.

Author details
[1]Clinical Medical Research Center, Guangdong Provincial Engineering Research Center of Autoimmune Disease Precision Medicine, Shenzhen Engineering Research Center of Autoimmune Disease, The Second Clinical Medical College of Jinan University, Shenzhen People's Hospital, Shenzhen 518020, Guangdong, China. [2]Institute of Nephrology and Blood Purification, The First Affiliated Hospital of Jinan University, Jinan University, Guangzhou 510632, China. [3]Shenzhen Far East Women & Children Hospital, Shenzhen 518000, Guangdong, China. [4]Department of Medicine Nephrology, Medical Faculty, Mannheim Heidelberg University, 68167 Mannheim, Germany. [5]Guangxi Key Laboratory of Metabolic Disease Research, Central Laboratory of Guilin NO. 924 Hospital, Guilin 541002, China.

Accepted: 10 August 2022
Published online: 25 September 2022

Reference

1. Wu H, Liu F, Shangguan Y, Yang Y, Shi W, Hu W, Zeng Z, Hu N, Zhang X, Hocher B, Tang D, Yin L, Dai Y. Integrating spatial transcriptomics with single-cell transcriptomics reveals a spatiotemporal gene landscape of the human developing kidney. Cell Biosci. 2022;12:80. https://doi.org/10.1186/s13578-022-00801-x.

Publisher's Note

Springer Nature remains neutral with regard to jurisdictional claims in published maps and institutional affiliations.